JOURNAL OF GEOPHYSICAL RESEARCH, VOL. 102, NO. E8, PAGES 19,371–19,382, AUGUST 25, 1997

SO_2-rock interaction on Io
2. Interaction with pure SO_2

D. S. Burnett,[1] Julia Goreva,[1] S. Epstein,[1] Susan L. Haldemann,[2] Mary L. Johnson,[3] and Alan Rice[4]

Abstract. A Na-S mineral on the surface of Io is required to be the source of the famous atomic cloud. SO_2 is a confirmed atmospheric and surface constituent, and because of the rapid volcanic resurfacing rate, the SO_2 is buried within the crust, where at least occasionally, over many cycles of burial and eruption, it must contact silicate materials at midlevel crustal temperatures. Surface interaction experiments were performed for a wide variety of silicate compositions showing that interaction products of these with SO_2 could be observed at 1123 K on laboratory timescales, even in the absence of external redox agents. Not all experiments produced deposits that could be studied by scanning electron microscopy; some required the greater sensitivity of photoelectron spectroscopy (XPS). Characterization of the alteration products by XPS showed that both oxidized and reduced sulfur species were formed, indicating that a disproportionation mechanism producing a sulfate and a reduced S species although smaller amounts of interaction leading to Na_2SO_3 formation cannot be ruled out. The reduced sulfur species is best explained as elemental S which was independently documented for two compositions. Scanning electron microscopy studies for those compositions where reaction was extensive enough to be observed showed (1) Na_2SO_4 for a soda-lime composition, (2) a mixed Na-Ca-sulfate liquid and $CaSO_4$ for AbAnDi and a chondrule glass composition, and (3) Fe-sulfate for a natural obsidian. Infrared spectroscopy for the soda-lime glass composition showed peaks best explained by Na_2SO_4. We conclude that SO_2 disproportionation as well as direct formation from SO_3 under oxidizing conditions can produce $Na2SO_4$ by interaction of SO_2 with silicates on Io, but Ca and Fe sulfates may form preferentially in more basaltic compositions. As highly oxidizing conditions may be unlikely for Io, the disproportionation mechanism may be more competitive on Io than it is in laboratory experiments. Very low rates of Na_2SO_4 production are required to supply the Io atomic cloud, so the interaction processes can be very inefficient.

Introduction

We have initiated a program of laboratory simulations aimed at identifying the nature and origin(s) of the Na-bearing phases on the surface of Io. Voyager showed that the inner Jovian magnetosphere contains a major population of energetic ions of O, S, and Na derived from Io [*Vogt et al.*, 1979; *Belcher*, 1983; *Krimigis and Roelof*, 1983; *Schardt and Goertz*, 1983; *Gehrels and Stone*, 1983]. Subsequent Earth-based observations and Galileo data to date have not changed this basic conclusion. Assuming that the ions arise from species derived by sputtering of the surface, the absence of Si in the torus (or in the atomic cloud; M. Brown, private communication, 1996) indicates that the outer surface layers are not silicate. Silicate flows occur [*Blaney et al.*, 1995]; however, given 0.1-1 cm/yr resurfacing rates, they may occupy only a small fraction of the area of the planet before being covered up with S and SO_2 deposits. However, large areas of silicates can be present on the surface if atmospheric SO_2 column densities are always sufficiently thick to hold back sputtered Si species.

Although it is widely accepted that the atmosphere of Io is patchy [e.g., *Spencer and Schneider*, 1996], it is unclear whether there are large areas of very low density patches from which significant quantities of sputtered atoms and molecules can escape. If species sputtered from the surface never penetrate the SO_2 atmosphere, then there must always be a large concentration of Na-rich, nonsilicate, aerosol particles at exospheric heights in order to account for a continuously present atomic Na cloud and torus Na ions by sputtering of the aerosol particles. Particles, at least of S and/or SO_2, must exist to explain why the plumes are visible. It is not known whether volcanic mass ejection rates can supply a large steady state density of high-altitude Na-rich particles. It is simpler to assume that sputtering occurs from the surface through the low-density patches in the atmosphere; nevertheless, regardless of whether sputtering occurs from surface or atmosphere, the major point remains unchanged: Na must arise from Na-S or Na-O compounds, not silicates. This interpretation has been implicit in essentially all post-Voyager discussions of Io surface composition. Even if Na were brought to the surface as Na atoms or as Na-O compounds [*Fanale et al.*, 1982], crustal recycling will convert these to either Na_2SO_4 or Na sulfides;

[1]Division of Geological and Planetary Sciences, California Institute of Technology, Pasadena.
[2]Department of Chemistry, University of California, Los Angeles.
[3]Gemological Institute of America, Santa Monica, California.
[4]Division of Physics, Mathematics, and Astronomy, California Institute of Technology, Pasadena.

Paper number 97JE00718.
0148-0227/97/97JE-00718$09.00

thus, unless radiation chemical reactions with the surface dominate Ionian Na chemistry, the present Na cloud arises from a Na-S phase [*Burnett*, 1995].

Unlike Io, the Na atmospheres of the Moon and probably Mercury are derived from silicate materials. These planets may have Na-rich vapor deposit outer layers produced by impact deposition from which Na atoms are preferentially "desorbed" by solar UV or higher energy photons. The densities of these Na atmospheres are much less than that of Io. Moreover, because of the rapid resurfacing rate, impact deposition cannot account for the Io Na cloud.

The sputtering process is not highly selective. If sputtering steady state is attained, the composition of the sputter products will be identical to the bulk composition of the substrate sputtered. For Io, it is probably unlikely that a sputtering steady state is attained given the high resurfacing rate. In this case the sputter product composition can differ from the bulk; however, such preferential sputtering effects are worth only a factor of 2-3 [*Feldman and Mayer*, 1986, section 4.7] and could not explain the absence of Si from the torus if the Na arises from silicate material. The absence of cations other than Na (and K) in the Io torus permits the unique conclusions made above.

Both theoretically and observationally (in meteoritic and planetary materials), Na is found in silicate minerals, and it is a good assumption that this was also the case in the input materials to Io. Ionian processes have extracted the Na, and it is these processes that we seek to determine.

In a previous study [*Johnson and Burnett*, 1990], we showed that the interaction of liquid elemental S with silicate glass at temperatures of 1100-1200 K would produce Na sulfides as alteration products, most likely Na_2S_5 in our experiments. The Na sulfide alteration products could be entrained in S magmas (or dissolved at higher temperatures) and transported to the surface during S volcanism. The issue arises, however, whether elemental S is required to explain the Na-rich surface of Io. Although widely accepted by almost all workers [e.g., *Moses and Nash*, 1991], elemental S is not a confirmed surface constituent of Io [*Hapke*, 1989; *McEwen and Lunine*, 1989]. Consequently, it is important to test for alternative origins for Na surface compounds which do not require elemental S.

In contrast to S, SO_2 is a confirmed atmospheric and surface constituent [e.g., *Nash et al.*, 1986, *Ballester et al.*, 1990, *Lellouch et al.*, 1990, *Trafton et al.*, 1996]. *Johnson and Burnett*, [1993] showed that, under highly oxidizing conditions, SO_2 reacted extensively with a wide variety of silicate compositions at 1123 K (mid level crustal temperature for Io). In all experiments, extensive sulfate surface deposits were found, but the nature of the sulfate changed systematically with the silicate Ca/Na ratio. Mixtures of $CaSO_4$ and Na-rich sulfate were formed from basaltic compositions having higher Ca/Na, but only alkali-rich sulfates formed from more granitic (low Ca/Na) compositions. For crystalline albite and an albite-orthoclase eutectic glass composition, K and Al-rich sulfates were formed. The presence of SO_3 on Io has been proposed by *Khanna et al.* [1995] based on Voyager thermal emission spectra. If true, this would make the *Johnson and Burnett* [1993] study more relevant, but the details of SO_3 destruction during crustal recycling would be important. A thick photochemically derived, non-condensable O_2 atmosphere has been proposed [*Kumar and Hunten*, 1982; *Lellouch et al.*, 1990]; however, the need for any permanent atmosphere on Io has been questioned by others [e.g. *Johnson and Matson*, 1989] and high column densities of O_2 are not predicted in recent photochemical models [*Summers and Strobel*, 1996].

For terrestrial basalt compositions, the stable S phases and corresponding silicate liquid solubilities have been relatively well studied in experiments over a range of oxygen fugacities and temperatures [e.g., *Carroll and Rutherford*, 1985, 1987; *Carroll and Webster*, 1994]. For conditions more reducing than about the NiNiO buffer, reduced S predominates, both dissolved in the liquid and as FeS. Although there is undoubtedly a wide range of redox conditions on Io, the predominance of SO_2 probably indicates relatively oxidizing conditions and/or very low concentrations of Fe in upper crustal silicate magmas. In any case, *Johnson and Burnett* [1993] represent an end member study.

However, there are also possible redox-independent mechanisms for the interaction of SO_2 with silicate materials (SO_2 alteration) producing Na-S compounds. These are the focus of this study. We report studies of "direct" interaction mechanisms with pure SO_2 which do not involve external redox agents: SO_2 disproportionation, which can be represented schematically as

$$(R1) \qquad 3\ SO_2 + 2\ [Na_2O] = S + 2\ Na_2SO_4$$

or sulfite formation:

$$(R2) \qquad SO_2 + [Na_2O] = Na_2SO_3$$

where square brackets indicate species in silicate glasses. For the conditions of our experiments, Na_2SO_3 as a pure compound is stable with respect to decomposition. In place of elemental S in (R1), it is possible to have Na sulfide (Na_2S_x) or FeS in iron-bearing samples. Also variations on (R1) producing $CaSO_4$ or silicate-sulfate liquids are possible.

Experiment

Reaction products were characterized by scanning electron microscopy (SEM), photoelectron spectroscopy (XPS), and infrared spectroscopy. Optimum sample preparation differs for these techniques; consequently several sets of experiments have been carried out with the common theme of exposing silicate materials to SO_2 gas at 1123 K (850°C), although some experiments were run at 1023 and 923 K. Samples used (Table 1) were natural albite (from Amelia, Virginia), synthetic albite-orthoclase eutectic glass (AbOr), natural Mono Craters obsidian, commercial soda-lime glass, synthetic albite: anorthite: diopside glass (AbgAnDi), synthetic chondrule mesostasis glass (Chon), and natural Kilauea alkali basalt (KAB).

With albite as the source of Na_2O it can be predicted from standard free energy data that reactions (R1) and (R2) above should not occur. Thus the albite experiments serve the purpose of blank runs.

For SEM and XPS characterization, the samples were cut into small pieces with a diamond saw and cleaned by ultrasonic agitation in spectroscopic-grade methanol. Samples were stored in Al foil cleaned by the same process. Two sample slices were used for each experiment (a smaller piece for SEM analysis and a larger piece for XPS). In most runs a slice of Optosil silica glass was included as a control. Two experiments were carried out in the presence of reagent Cu metal. For the infrared studies, finely powdered samples of the same compositions were prepared using an agate ball mill.

Table 1. Starting Materials

	Oxides. Wt %							
Name	Na_2O	MgO	Al_2O_3	SiO_2	CaO	K_2O	FeO	Other
Albite [a]	11.07	0.04	19.65	67.84	0.00	0.29	0.04*	0.86 H_2O
AbOr [b]	5.7	-	18.8	66.4	-	8.7	-	0.43% Sb_2O_3
Obsidian [c]	3.80	-	12.32	76.45	0.52	4.75	1.02*	0.06 TiO_2, 0.06 MnO
Soda-lime [d]	15	4	1	73	7	tr	tr	tr Ti O_2
AbAnDi [e]	9.5	1.9	19.2	64.8	4.6	-	-	
Chon [f]	6.39	8.11	17.31	62.56	5.51	-	-	
KAB [g]	2.26	7.23	13.8	49.94	11.40	0.52	8.58	2.71 Ti O_2, 2.82 Fe_2 O_3, 0.17% MnO

* All Fe calculated as FeO.

[a] Amelia albite, Ward's Scientific Establishment, Inc. Composition from *Deer et al.* [1966, p. 324].

[b] Albite-Orthoclase eutectic composition, Corning Glass 1298, courtesy E.M. Stolper.

[c] 1340 A.D. Eruption, Mono Craters, CA; North Coulee obsidian, courtesy *Newman et al.* [1988].

[d] Commercial "soft glass" slides, VWR 48318-009.

[e] Albite:Anorthite:Diopside 8:1:1 glass, Corning experimental glass 608 PEM, made by L.R. Pinckney.

[f] Chondrule mesostasis composition glass, Corning experimental glass 608 PEL, made by J. Fine, courtesy R.C. Wiens.

[g] Kilauea alkali basalt, August 1971 flow, collected by D.S. Burnett, August 30, 1973; composition assumed to be that of USGS standard powder BHVO-1 [*Gladney and Roelandts*, 1988].

Silicate samples were sealed with SO_2 gas in 9mm, i.d. silica glass capsules. At the temperatures of our experiments, we found that reaction of the samples with the silica glass capsules was not important. The vacuum line was evacuated, then isolated from the Hg diffusion pump, and SO_2 admitted to about 1 atm pressure. The SO_2 was then trapped into a reservoir with liquid N_2, and any residual gas pumped away. At this stage some residual noncondensible gas was always observed on the manometer before pumping. The desired aliquot of SO_2 was taken from the reservoir, trapped onto the sample, and then pumped on to remove any residual non-condensable gas, although none could be observed on the manometer at this point. All water in the system should be trapped in the reservoir at this point, and all O_2 should have been pumped away. System pressures at this point were less than 5-10 microns. With the SO_2 still frozen, the reservoir valved off, and the sample open to the vacuum pump, the sample capsule was sealed from the vacuum line. Earlier experiments with albite and soda-lime glass using a less elaborate sealing-off procedure showed extensive reaction [*Johnson and Burnett*, 1991]. This was a surprising result because possible alteration reactions involving albite are not possible thermodynamically. A possible explanation was the presence of a small amount of O_2 in the sealed capsule; consequently, the more elaborate sample sealing procedure described above was adopted. An albite experiment using the above sealing procedure showed no detectable reaction, even with XPS, the most sensitive technique.

Amounts of SO_2 gas loaded corresponded to 3-5 pressure at 1123 K.

Control experiments were performed, in which silicates, both slices and powders, were heated in evacuated capsules without SO_2 present.

The SO_2-sealed capsules were placed in a 1123 K horizontal furnace, 7-26 days for most experiments, then quenched in air. One sample of the AbAnDi glass was examined after being in the furnace for 438 days. The products were visually examined before the capsules were opened. On opening, the presence of unreacted SO_2 was confirmed by sniffing; in all cases, SO_2 was detected. In the initial experiments the small piece of sample was mounted and carbon-coated for SEM characterization. The larger piece was wrapped in cleaned Al foil and held for XPS study. Later, improved procedures were adopted in which the time between opening and XPS analysis was held to a minimum (see Results section). Surface reaction products were identified with a CAMSCAN series II instrument using a backscattered electron detector and an energy dispersive Si(Li) X ray detector. Because the sample slices tended to deform on heating and because the deposits form a rough coating, only qualitative SEM analyses have been performed.

XPS spectra were obtained both with a highly modified VG instrument and, more recently, with a Surface Science Corp. M-probe located in the Caltech Beckman Institute. The VG instrument analyzed a spot that was roughly 1x1 cm. The M-probe has better spatial resolution down to about 100 microns, permitting spectra to be taken at different submillimeter-sized spots on the silicate surface.

The powdered samples for infrared characterization were heated for 26 days at 1123 K. After visual inspection and opening the capsule, aliquots of 3-10 mg of powdered silicate were sampled for infrared characterization. The products showed a wide range of sintering, ranging from essentially no reaction for the powdered albite to melting for the soda-lime glass and Mono obsidian. The aliquots were ground in a cleaned stainless steel mortar, mixed with about 140-160 mg of KBr, and pressed into a ~1 cm diameter pellet. Transmission infrared spectra were obtained with a Nicolet Fourier transform infrared spectrometer using a Hg-Cd-telluride detector. Spectra were obtained down to ~500 cm^{-1} (20 microns).

Results

Photoelectron Spectroscopy

In XPS spectra, peaks are produced by photoelectric effect interactions occurring in the outer few monolayers of a surface, and these can be identified using known electron binding energies of specific elements. Relatively large sample areas are needed, although the M-probe instrument allowed submillimeter size regions to be studied. Only major elements can be seen (greater than several percent), but light elements such as C and O can be analyzed.

Figure 1 shows a typical spectrum for the electron binding energy range of 145 to 170 eV. The large peak at 151 eV cor-

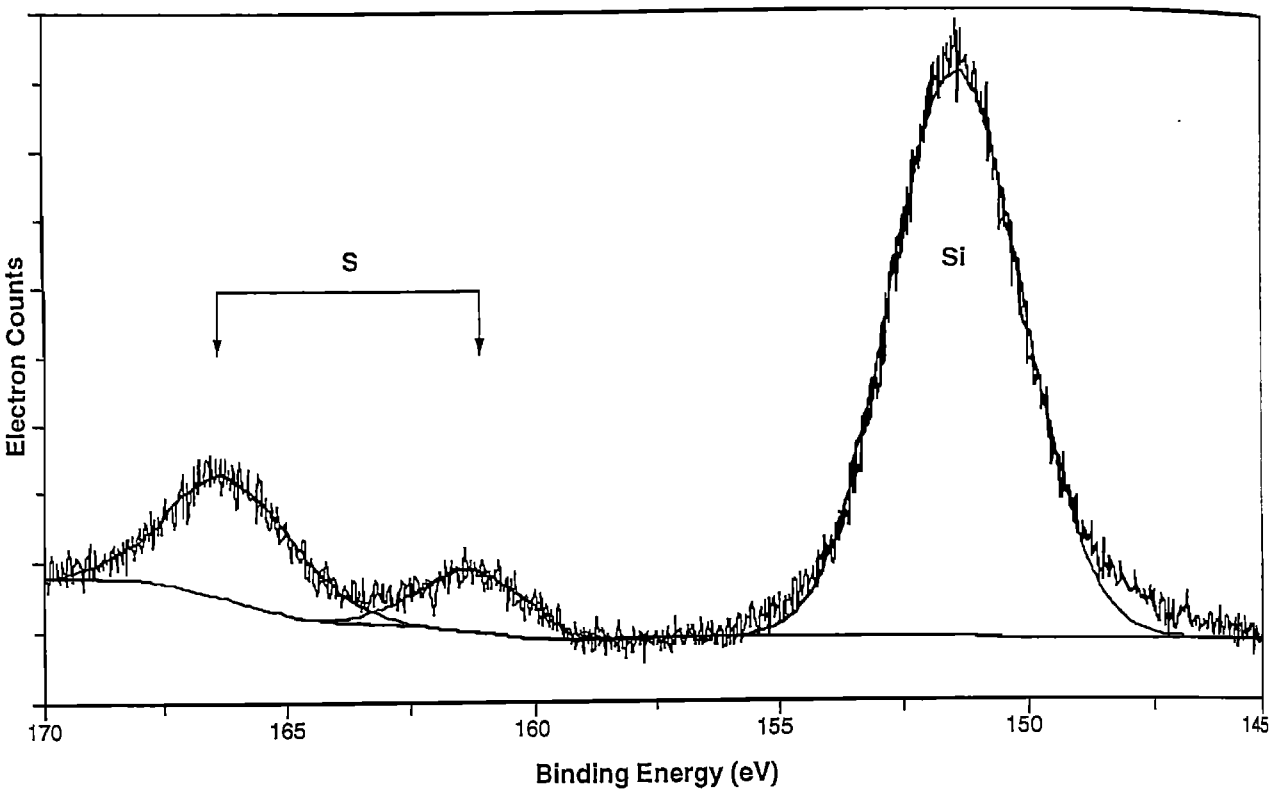

Figure 1. Photoelectron spectrum of sample of Mono Craters obsidian exposed to SO_2 for 26 days at 1123 K. The more intense S 2*p* electron peak at 166 eV is due to an oxidized S species. The weaker S 2*p* peak at 161 eV corresponds to reduced S. The two-peak spectrum indicates SO_2 disproportionation with the formation of Na_2SO_4 or $CaSO_4$. Overall, the reduced peak is best described as elemental S with the lower intensity due to S volatility. The relative intensity of the S and Si peaks is a rough measure of the degree of reaction.

responds to Si 2s electrons and is a very useful reference peak for comparison with the S lines. The higher binding energy peaks correspond to a doublet of S 2p lines, the one at 161 eV corresponding to reduced S and the one at 166 eV to an oxidized S species. For the following reasons the identification of the S peaks is firm: (1) Spectra of Na_2SO_4 and S support the oxidized and reduced S assignments, although variable amounts of sample charging prevent precise measurements of binding energies. (2) Inspection of tables of electron binding energies and Auger lines shows no plausible alternatives. (3) The measured separation of the peaks (4.8 eV) agrees with that expected between oxidized and reduced S species from compilations of XPS chemical shifts for S compounds [e.g., *Wagner and Muilenberg*, 1979]. Between Na_2SO_4 and elemental S, a chemical shift of 4.8 eV is expected; between Na_2SO_4 and Na_2S, 7.0 eV would be expected, but the peak positions for Na_2S_x approach that of elemental S as x increases; consequently, based on XPS chemical shifts, we are only confident of ruling out Na_2S as the reduced species (but not Na_2S_3). (4) When the spectra of the same sample have been followed over time (for periods up to 1 year), the reduced S peak disappears. We interpret this as a combination of oxidation of the reduced S species and sublimation of elemental S in vacuum [*Nash and Moses*, 1988], but both mechanisms are a mark of reduced S.

The summary of XPS results in Table 2 shows that a two-peaked spectrum was observed for all samples except AbAnDi The two peak XPS spectrum is strong evidence for the predominance of the disproportionation alteration mechanism (R1),

Table 2. Summary of XPS Results

XPS Sample	Atomic	XPS Spectra	SEM
Albite	0	nothing	no reaction
AbOr Eutectic Glass [b] (SO_2-5t)	0	two peaks	no reaction
Obsidian [a] (SO_2-6b)	0.08	two peaks	Fe-S phase
Soda-lime Glass [c] (SO_2-4c)	0.2	two peaks	Na-S
Ab gAnDi Glass [a] (SO_2-6e)	0.27	oxidized only	Na-S+Ca-S
Chondrule Glass [b] (SO_2-5h)	0.48	two peaks	Ca-S
KAB Alkali Basalt [b] (SO_2-6f)	3	two peaks	no reaction

[a] 5-10 minute air exposure.
[b] Opened in N_2; no air exposure.
[c] Extensive air exposure prior to XPS analysis.

where the products are a reduced sulfur species and sulfate; thus two peaks are expected for (R1), whereas only one peak is expected for (R2). The reduced S peak could correspond to elemental S or to a Na sulfide, although the literal interpretation of the chemical shift is elemental S.

In the case of the soda-lime composition, elemental S is independently confirmed as the reduced S product: The powdered soda-lime sample experiments prepared for IR studies contained a yellow gas on removal from the furnace. The yellow gas condensed to a yellow liquid then a white solid. The white solid showed no Na on XPS examination and pumped away in the XPS vacuum system. Some other samples showed evidence for elemental S on SEM examination (next section).

For sulfite formation (R2) only one oxidized S peak would be observed. For the Fe-bearing natural rock compositions, oxidation of SO_2 by Fe_2O_3 or Fe_3O_4 (magnetite) would also produce only a single oxidized peak if

(R3a) $3\ SO_2 + 4\ [Fe_2O_3] = 6\ [FeO] + Fe_2(SO_4)_3$

(R3b) $3\ SO_2 + 4\ Fe_3O_4 = 10\ [FeO] + Fe_2(SO_4)_3$

(R3c) $[Na_2O] + SO_2 + [Fe_2O_3] = Na_2SO_4 + 2\ [FeO]$

(R3d) $[Na_2O] + SO_2 + Fe_3O_4 = Na_2SO_4 + 3\ [FeO]$

where the square brackets signify components in silicate glasses. Reactions analogous to (R3c) or (R3d) forming $CaSO_4$ are also possible. Magnetite is relatively abundant in the obsidian and is a trace mineral in the alkali basalt glass. However, with two XPS peaks observed, there is no evidence for any of the (R3) reactions. We of course cannot rule out that both disproportionation and reactions (R3) or (R2) contribute to the observed reaction products. Variations on (R3) with elemental S as the product would produce two XPS peaks and are considered in connection with the SEM obsidian studies.

The oxidized S peak position cannot be used to decide between sulfite and sulfate because of local sample charging, despite the use of an electron flood gun. Sample charging shows clearly in the data on the Si 2s line where the peak position varies from sample to sample from 149 to 157 eV and the peak position shifts with the voltage of the electron flood gun. Evidence for differences in the amount of charging for different points on the same sample were also found.

The susceptibility of the reduced S peak to oxidation also shows that XPS analysis needs to be done promptly after opening the capsules. In the initial series of experiments the SEM characterization was done first, and periods of weeks elapsed before XPS analysis. Thus, only 2/6 of these samples showed the double-peak spectrum. A second round of experiments was performed with at most 10 min exposure to air prior to placing in the XPS vacuum chamber. As the ultimate experiment, three samples (Chon, AbOr, KAB) were opened in a dry N_2 atmosphere and introduced directly into the XPS chamber vacuum system. The relative amounts of reduced and oxidized sulfur were not significantly greater; consequently, we conclude that air exposure of the order of ~10 minutes does not appear to produce the oxidized S peak. The results summarized in Table 2 are for the minimal air exposure samples.

A complication to the interpretation of the XPS reduced S peak as elemental S is that, at 1123 K and $P(SO_2) \sim 3$ atm, elemental S is a gas. As the sample is removed from the furnace, S will condense. If the condensation were uniform on all surfaces, then it should also be present on the slices of SiO_2 glass included as controls in all experiments. The SiO_2 glass controls have been systematically examined by XPS. No S peaks were detected, but assuming uniform condensation, this can be explained if only about 10^{-4} of the original SO_2 has reacted. The reduced S peak on the samples then implies either (1) the interpretation of the reduced S peak as elemental S is incorrect, (2) S and sulfates form an intimate reaction product mixture that traps S, (3) condensation preferentially occurs on sample surfaces rather than on SiO_2 glass (chemisorption?), or (4) a fraction of the S produced by disproportionation is trapped in cracks, where it volatilizes very slowly. As there is strong independent evidence for S for some samples, explanation 1 seems unlikely. The other alternatives are not mutually exclusive. As discussed below, there is support in the SEM data for explanation 4. Greater volatility, either of S or Na_2S_x can explain why much larger peaks of oxidized S were always observed, even in samples never exposed to air.

The interpretation of the single peak AbAnDi spectrum is best done in the context of the SEM data below.

As expected, no XPS S peaks were observed for albite experiments. Similarly, the SiO_2 glass slices included as controls in most experiments have been systematically checked with no S peaks. These experiments are a control on possible reactions with contaminants, which is a concern given the high sensitivity of XPS to surface contamination. The dominant impurities are reduced C compounds and water. (The natural rock samples have 0.1-1% H_2O.) Water is stable in the presence of SO_2, and small quantities should not be an issue except possibly to promote disproportionation reactions by bisulfate (HSO_4^{2-}) formation (compare *Johnson and Burnett* [1993]). Reduced, polymerized C (here taken as C_2H_2) should be destroyed by SO_2:

$$2C_2H_2 + 5SO_2 = 4CO_2 + 2H_2O = 5S$$

The lack of XPS S peaks for the albite and SiO_2 glass control sample data show that the ubiquitous observation of a reduced XPS S peak for the silicate glass samples cannot always be due to the presence of organic contaminants.

SEM Observations

A summary of SEM observations is given in Table 3. Those individual runs which yield a significant conclusion are discussed below in order of increasing Ca/Na, as this ratio was found to be important by *Johnson and Burnett* [1993], reflecting the competition between $CaSO_4$ and Na_2SO_4 as the oxidized S species.

The AbOr and alkali basalt (KAB) samples had no SEM-observable reaction products. Interestingly, these samples are the extremes in terms of Ca/Na (ABOr, Ca/Na=0; KAB; Ca/Na=3).

Obsidian (Ca/Na=0.08). Amounts of observable reaction products were very small. No Na-S phases were found. On a sample from experiment SO_2-6b, small amounts of an Fe-S phase were found. Larger amounts were found on sample SO_2-6d. Variable amounts of Cl were seen with all spectra of this phase. No evidence for high reflectivity sulfides was found upon optical examination of the reacted surfaces, indicating that the Fe-S phase was an iron sulfate rather than FeS. Small pieces of an Fe-S phase were also seen on one of the AbAnDi samples. There is no Fe in this sample, so the iron sulfate must be a contaminant in this case. However the iron sulfate

Table 3. SEM Results

Run	T, K	Time, days	Silicate	Results
SO_2-1	923	21	Albite	no reaction
			Soda-lime	Na-S phase
SO_2-21	923	21	Albite, Cu	no reaction
SO_2-22	923	21	Soda-lime, Cu	Na-S phase
SO_2-25	923	21	Soda-lime, Cu	Na-S phase
SO_2-4a	1023	56	AbOr	XPS only
			Soda-lime	XPS only
SO_2-4c	1123	7	AbOr	no reaction
SO_2-4d	1123	7	AbOr	no reaction
			Soda-lime	Na_2SO_4
SO_2-5b	1123	7	Chon	Ca SO_4
SO_2-5h	1123	26	Chon	XPS only
SO_2-5t	1123	26	AbOr	XPS only
SO_2-6a	1123	7	AbAnDi	Ca SO_4
SO_2-6b	1123	26	Obsidian	rare Fe-sulfate
SO_2-6c	1123	7	KAB	no reaction
SO_2-6d	1123	7	Obsidian	Fe-sulfate
SO_2-6e	1123	438	AbOrDi	elemental S
SO_2-6f	1123	26	KAB	XPS only
SO_2-6g	1123	7	AbAnDi	Na-Ca-S (liquid?)

in the obsidian samples appears to be real because the amounts are much larger and the sulfate appears to be in, as opposed to just sitting on, the surface Thus our best interpretation of the two peak XPS spectrum for the obsidian (Figure 1) is that the reduced species is S and the oxidized peak is an Fe-sulfate:

(R4) $2\,[FeO] + 3\,SO_2 = S + 2\,FeSO_4$

$2\,[Fe_2O_3] + 9\,SO_2 = 3\,S + 2\,Fe_2(SO_4)_3$

$2\,[FeO] + 5\,SO_2 = 2\,S + Fe_2(SO_4)_3$

$2\,Fe_3O_4 + 8\,SO_2 = 2\,S + Fe_2(SO_4)_3$

where square brackets indicate species dissolved in silicate glass.

Soda-lime glass (Ca/Na=0.2). Experiment SO_2-4d had about 60% surface coating of 10 micron crystals of a Na-S phase with minor amounts of K, Ca, and Al (Figure 2). There is some suggestion of two generations of Na-S phase formation. The SEM X-ray spectra only show Na and S; distinguishing Na_2SO_4, Na_2SO_3, or Na_2S in these samples is not possible, but Na_2SO_4 is required to account for the oxidized S species in the two-peak XPS spectrum. Below the large crystals there is a

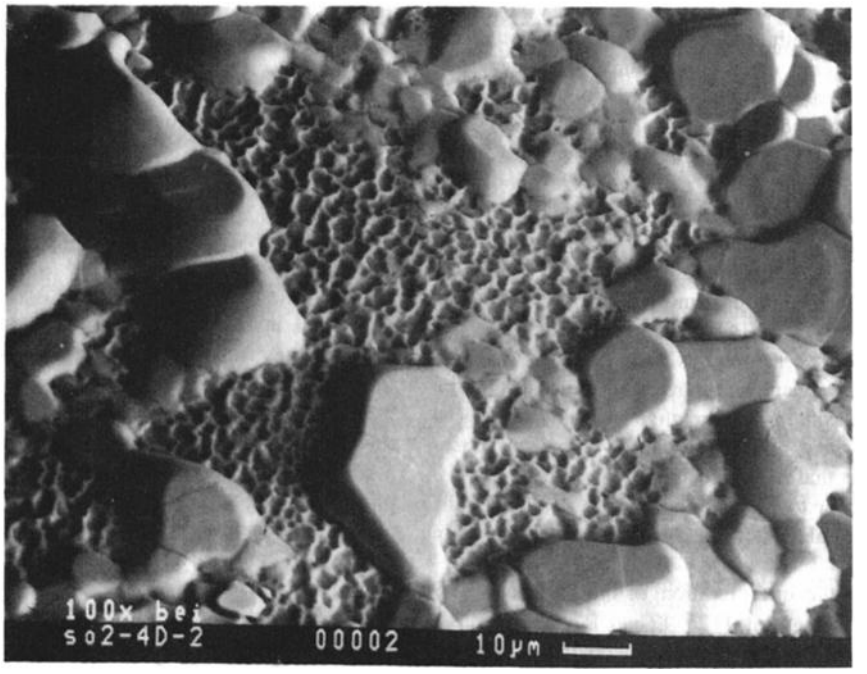

Figure 2. SEM image of SO_2-4d (soda-lime) reacted surface, showing large rounded crystals of Na_2SO_4, and puckered surface of high-relief sulfate ridges and low areas filled by silica.

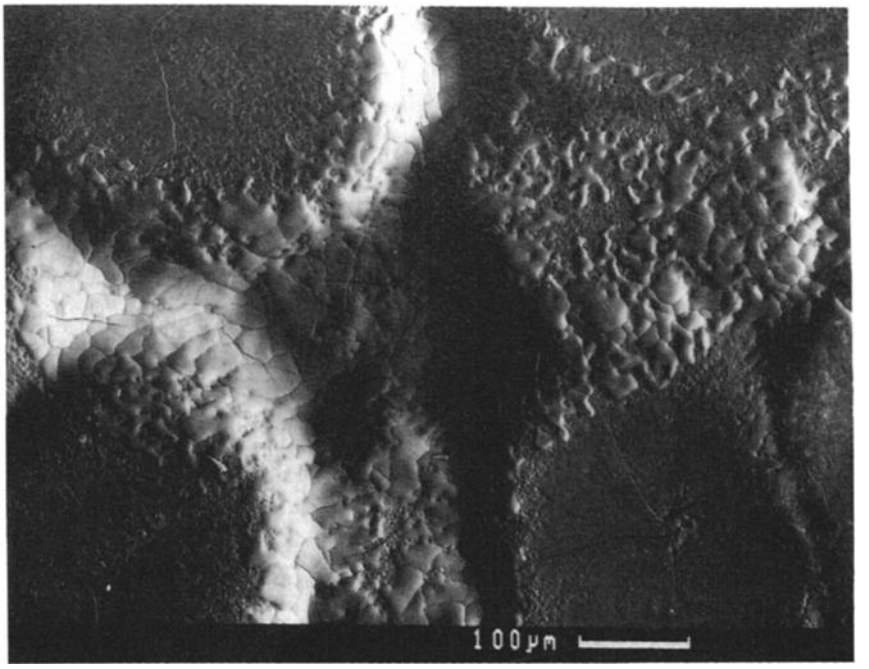

Figure 3. SEM image of SO_2-6g (AbAnDi) surface, showing large plateaus of silicate partially coated with droplets of (Na,Ca) sulfate (liquid?).

honeycomb structure of an apparently early-formed Na_2SO_4. The spectra of the interstices of the honeycomb show only Si, possibly from surface SiO_2 crystallization due to a combination of devitrification and of the reactions producing the Na-S phase.

SO_2-1 (soda-lime; 923 K, 21 days) was an early experiment, probably with some air contamination, so the phase formed is undoubtedly Na_2SO_4 in this case. The glass surface was extensively devitrified, with Na_2SO_4 present as ~40 micron rings of 3 micron crystals. Somewhat surprisingly, considering the oxidizing conditions, the amount of Na_2SO_4 formation was small, roughly 1% surface coverage. It appears that the rate of reaction, at least for the soda-lime glass, decreases rapidly with temperature.

AbAnDi glass (Ca/Na=0.27). Results for this sample are complex. Experiment SO_2-6g showed a plateau and valley structure of silicate host glass with droplets and stringers of a (Na,Ca,S) phase on the plateaus (Figure 3). The texture is suggestive of a mixed sulfate liquid. In contrast, a nominally duplicate sample, SO_2-6a has a surface almost totally covered with euhedral crystals of a Ca-S phase, almost certainly anhydrite in view of the oxidized S XPS peak on this sample. A major search for coexisting Na_2SO_4 was unsuccessful. A third AnAbDi sample (SO_2-6e) was left in the furnace at 1123 K for over a year. The XPS spectrum of the large piece of experiment SO_2-6e shows only a weak oxidized S peak; no S phase was seen on SEM examination of this piece. SEM examination of the small piece of SO_2-6e revealed a dusting of elemental S droplets on the surface and some cracks filled with elemental S. It is likely that, for unexplained reasons, the elemental S on the large piece was completely pumped off in the XPS vacuum, unlike all other samples, explaining why the AbAnDi samples are unique in having only a single XPS peak. The SEM samples are C-coated, inhibiting S volatilization. Moreover, as discussed in the XPS section, it is surprising that any elemental S peak could be seen in the XPS. Consequently, it is all other samples that are anomalous. The AbAnDi samples are more "normal" in this sense. The elemental S observed on the SEM shows that SO_2 disproportionation is the mechanism for this composition also in spite of only oxidized S XPS peaks being observed. SEM examination of a polished cross section of the small piece of SO_2-6e showed apparently all glass except for a very minor amount of plagioclase and diopside crystallization; however, Ca was depleted in the outer few microns, suggesting that some $CaSO_4$ was formed, although we have not been able to find it. Additional experiments will be required to understand the differences in the products from the present AbAnDi experiments; however, it is worth emphasizing that our experiments should be regarded as Io simulations as opposed to determinations of equilibrium phase assemblages. It is possible that $CaSO_4$ failed to nucleate in one experiment and the Na,Ca sulfate liquid formed instead, and that in the year experiment the $CaSO_4$ layer fell off and we failed to recover it.

Chondrule glass (Ca/Na=0.5). Experiment SO_2-5b shows tetragonal (or pseudotetragonal) silicate crystals of very roughly $NaCaMg_4Al_2Si_7$ relative cation proportions (clinopyroxene?). Minor amounts of 5 micron prismatic crystals of a Ca-S phase are also present (Figure 4). As an oxidized S XPS peak is observed, this phase is likely to be $CaSO_4$.

Experiments in presence of Cu metal. Experiment SO_2-25 (soda-lime, Cu metal; 923 K for 21 days) showed extensive reaction with almost complete surface coverage of 10 micron crystals of a Na-S phase (Figure 5). A duplicate run (SO_2-22) showed the same results. The overall layer thickness was about 4 microns with greater thicknesses along scratches in the glass. The Cu metal was almost completely reacted, forming both an interior oxide and an outer sulfide layer. We interpret the overall reactions as

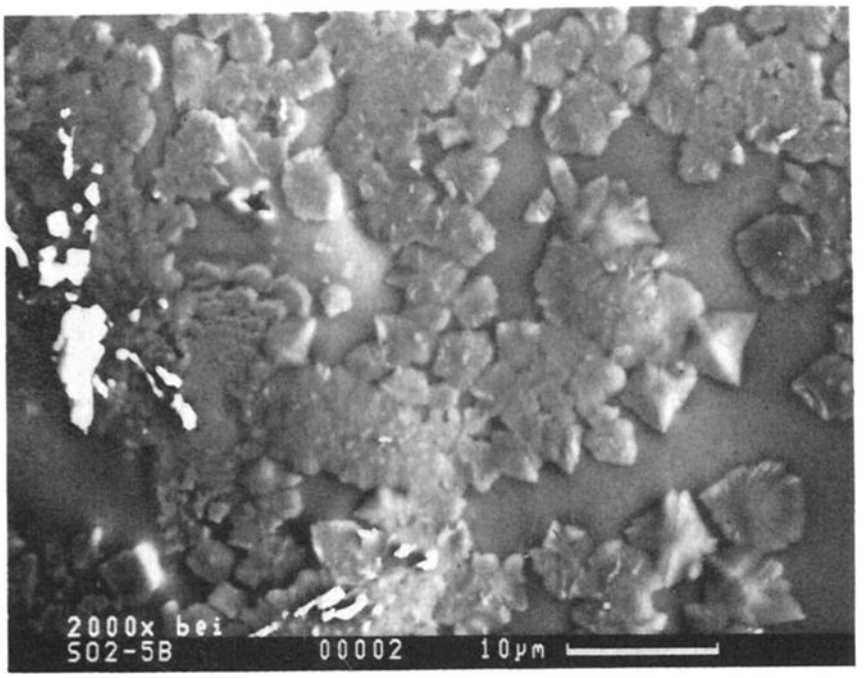

Figure 4. SEM image of SO_2-5b (Chon) surface, showing $CaSO_4$ (very bright, left side of figure) and flat tetragonal(?) plates of (Na,Ca,Mg,Al) silicate (bright rims show up in relief) on silicate matrix.

(R5) $2Cu + 3\ SO_2\ (g) + 2[Na_2O] = 2Na_2SO_4 + Cu_2S$

with the copper oxide reflecting

$$3Cu + SO_2 = 2\ Cu_2O + Cu_2S$$

as well as some direct air oxidation (this was an early experiment prior to implementation of our improved sample sealing techniques). Here, square brackets refer to species dissolved in the silicate glass We have selected cuprous, as opposed to cupric, compounds because reaction (R5) does not go for the cupric phases. This is an interesting variation of disproportionation being driven by Cu acting as both an oxidizing and a sulfurizing agent with the formation of a stable sulfide phase. Even though Cu metal is unlikely on Io, this experiment is of interest because, in principle, Fe_2O_3 could play a similar role on Io. The reaction, analogous to (R5) would be

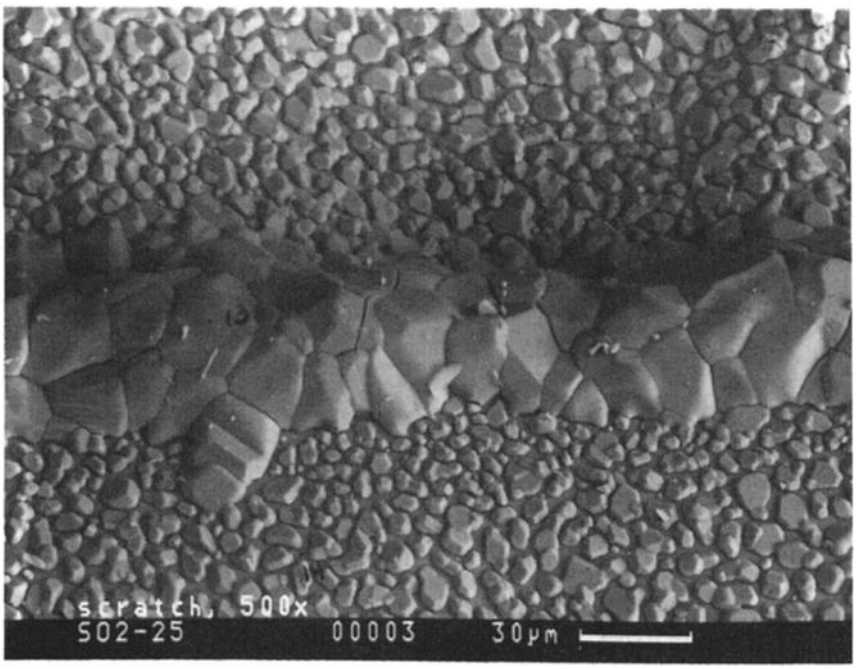

Figure 5. SEM image of SO_2-25 (soda-lime; Cu added) glass surface showing extensive coverage by Na_2SO_4 crystals. Line of large crystals covers a scratch on the original glass surface.

(R6) $[Fe_2O_3] + 9SO_2 + 7[Na_2O] = 7Na_2SO_4 + 2FeS$

where square brackets refer to products dissolved in the silicate glass. Although a complex reaction with two species (Fe^{+3} and S^{-4}) acting as reducing agents, the ferric iron and Na could be co-located in a silicate glass/lava on Io; moreover, two rather stable products are formed. However, the obsidian and KAB basalt samples, for which reaction (R3) is possible, show little reaction even at a 200° higher temperature, possibly because the Fe_2O_3 reaction rates are much lower.

Overall, the order of reactivity from XPS is soda-lime > AbAnDi > obsidian > Chon > basalt>AbOr. This order is generally consistent with the SEM results (Table 3). There are no obvious correlations of composition and reactivity.

In summary, the results of the SEM/XPS studies give fairly strong evidence for the disproportionation alteration mechanism (R1) which requires that sulfates (Na,Ca, or Fe) be the oxidized species; thus the phases identified with the SEM for experiments with two XPS peaks have been identified as sulfates (Figures 2-5). The reduced species has been identified as S for the soda-lime and AbAnDi samples and is likely for the others, although Na_2S_x cannot conclusively be ruled out. The observation of Ca-S products only with samples of higher Ca/Na is consistent with the data of *Johnson and Burnett* [1993], but iron sulfates were not observed in the earlier experiments.

Infrared Spectroscopy

The purpose of these experiments was to see if the presence of sulfates could be directly confirmed, ideally to characterize the proportions of Na_2SO_4 and $CaSO_4$, and to check for any sulfite formation along with disproportionation. Because of the relatively small amounts of reaction observed in the SEM/XPS studies, powdered silicate materials were used for this study, assuming that the larger surface areas would produce greater yields of reaction products. Aliquots of the reaction products were ground and pressed into KBr pellets. Pellets of the unheated starting materials were made as controls; however, presumably because of devitrification effects, the silicate background spectra are observed to be different for the heated and unheated samples. Consequently, a series of background simulation runs were made, identical to the SO_2 alteration experiments in every way except for the presence of SO_2.

Figure 6 compares absorbence spectra of background silicate (heated soda-lime glass) (Figure 6a) and soda-lime glass exposed to SO_2 at 1123 K (Figure 6b) with reference Na_2SO_3 (Figure 6c) and Na_2SO_4 spectra (Figure 6d). A major problem is that the silicate background spectra for different heated soda-lime glass samples are quite variable. This variability is not understood but it may mean that the amount of silicate devitrification differs when SO_2 is present than with SO_2 absent for the same thermal history. We have selected the background spectrum which looks most reasonable compared to the sample. Comparison of Figures 6a and 6b shows that most of the peaks in the sample can be accounted for by silicate features. A minor peak at 690 cm^{-1} in the silicate background spectrum does not appear in the sample spectrum. This is an example of the silicate background variability mentioned above. However, the major difference is a sharp, barely resolved doublet at 620 and about 645 cm^{-1}. The Na_2SO_4 reference spectrum (Figure 6d) shows peaks at the same positions although the ratios of the members of the doublet have a more unequal intensity ratio than Figure 6b. The Na_2SO_3 spectrum (Figure 6c) shows a narrow peak at 620 cm^{-1}, but this is a singlet; consequently, the doublet nature of the sample peak in Figure 6b is best described by Na_2SO_4. $CaSO_4$ (not shown) has sharp peaks at 590-610 (partially resolved doublet) and 670 cm^{-1}. Except for a small bump, there is no 670 cm^{-1} feature in the sample spectrum (Figure 6b), so only minor amounts of $CaSO_4$ can be present. The strong Na_2SO_4 absorption band at 1120 cm^{-1} (Figure 6d) might be present but is mixed with a broad silicate absorption feature peaking at ~1080 cm^{-1}. The analogous Na_2SO_3 absorption band is significantly lower, at 970 cm^{-1}. If most of the 620 cm^{-1} absorption in the sample (Figure 6b) were due to Na_2SO_3, then a significant peak should also be recognizable at 970 cm^{-1}, but except for a shoulder, no feature is found at 970 cm^{-1} in the sample spectrum. Given the high intensity ratio of the 620 and 970 cm^{-1} peaks in Figure 6c, even if all the observed 970 cm^{-1} shoulder in Figure 6b is due to Na_2SO_3, only a small fraction of the 620-645 cm^{-1} doublet in Figure 6b could be due to Na_2SO_3. The 970 cm^{-1} shoulder could be due to Na_2SO_3 or to a silicate devitrification feature. Nevertheless, the 620-645 doublet in the sample spectrum identifies Na_2SO_4 as the primary reaction product, consistent with the identification of Na-S phases in the SEM spectra and the expectation of sulfate for the disproportionation mechanism required to explain the XPS observations. Some Na_2SO_3 cannot be ruled out.

Spectra analogous to those obtained in Figure 6 have been obtained for the other five silicate glass compositions, but the results are inconclusive. Strong silicate peaks in the 470-640 cm^{-1} range (due to plagioclase?) mask sulfate features in the basaltic compositions (Chon, AbAnDi, KAB). Only a faint bump at 620 cm^{-1} is present in the obsidian spectrum. The infrared data confirm the presence of Na_2SO_4 for the soda-lime composition, but only for this sample.

Discussion

Summarizing the results, the SO_2 disproportionation mechanism (R1; see Introduction) forming reduced and oxidized sulfate peaks is demonstrated by the XPS spectra for all glass compositions except AbAnDi. The AbAnDi sample shows a single oxidized XPS peak, but S is observed on the SEM showing the disproportionation mechanism holds here also. For the sodalime composition, Na_2SO_4 and S are well documented as products. Similarly, $CaSO_4$ and S are documented for the AbAnDi and Chon samples with Fe sulfates formed from the obsidian. Some contributions to the SO_2-rock interaction process from sulfite formation cannot be ruled out, but there is no evidence supporting this mechanism.

If we combine the results of the present study and that of *Johnson and Burnett* [1993], there are two mechanisms to produce Na_2SO_4 by SO_2-rock interactions. Schematically, we can write these reactions as

(R7) $2[Na_2O] + 3SO_2 = S + Na_2SO_4$

and

(R8) $[Na_2O] + SO_3 = Na_2SO_4$

where the square brackets indicate that the Na_2O is contained in glass. Reaction (R7) is the redox-independent disproportiona-

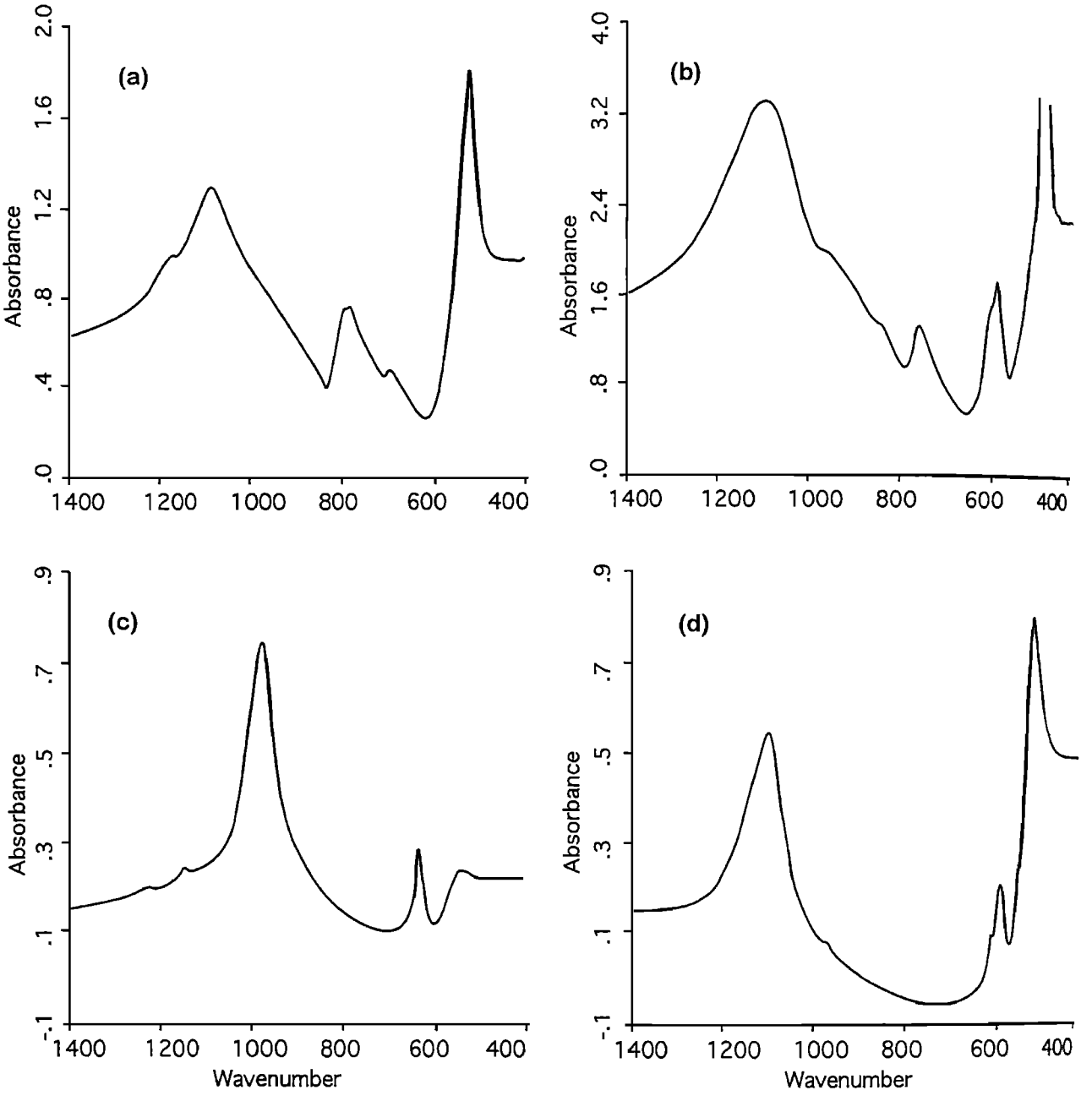

Figure 6. Infrared absorbance spectra (a) Soda-lime glass heated at 1123 K in vacuum. (b) Products from soda-lime glass heated in ~3 atm of SO_2. (c) Na_2SO_3 reference spectrum. (d) Na_2SO_4 reference spectrum. The doublet peak at 620-650 cm^{-1} and the absence of a 970 cm^{-1} peak in Figure 6b identifies the reaction product as Na_2SO_4. See text.

tion mechanism studied here; (R8) represents the prevalent mechanism under oxidizing conditions [*Johnson and Burnett*, 1993] where SO_3 would be important. Thus this study reinforces and generalizes the conclusion of *Johnson and Burnett* [1993] that SO_2-rock interactions need to be considered as a possible source for the Na seen in the Io atomic cloud.

The viability of SO_2-rock interactions relative to alternative mechanisms depends on upper crustal redox conditions and the nature of crustal recycling [*Burnett*, 1995]. It is clear, for at least the temperature of our laboratory studies (1123 K), that reaction (R8) is much more rapid than (R7), given oxidizing conditions. The rate of both reactions appears to drop rapidly with temperature. The possibility of an O_2 atmosphere for Io with $O_2 \sim SO_2$ [*Kumar and Hunten*, 1982, *Lellouch et al.*, 1990] was proposed because of the Pioneer 10 observation of a nighttime ionosphere which is unexpected because SO_2 should be condensed at nighttime temperatures. However, *Johnson and Matson* [1989] show that the region observed by Pioneer 10 included an active plume which could account for the ionosphere without the necessity of a noncondensible atmospheric component. In the most recent photochemical models [*Summers and Strobel*, 1996] the steady state O_2/SO_2 ratio is small beginning with an initial pure SO_2 atmosphere. A primordial O_2 atmosphere is unlikely because

(1) preferential O escape would cause it to evolve toward a steady state atmosphere with low O_2/SO_2, as modeled by *Summers and Strobel*, [1996], (2) there is no known geochemical mechanism to evolve an O_2 atmosphere from a silicate planet, and (3) although the reaction of S with O_2 at Io surface temperatures is probably negligible, if typical hot spot (sulfur lava lakes?) temperatures are ~400 K, then over the course of geologic time the hot spots would probably consume any primordial O_2 atmosphere. Thus highly oxidizing conditions on Io are unlikely, although the presence of oxidized S as SO_2 is equivalent to a reasonably oxidizing environment. On Io, reaction (R7) should dominate. The only effective way for (R8) to be important on Io is through the occurrence of SO_3 as a radiation chemistry by-product in the lower atmosphere. *Khanna et al.* [1995] interpret features in Voyager thermal emission spectra as being due to the presence of SO_3 which would give support to this possibility. It is unclear whether the results of *Khanna et al.* [1995] are quantitatively compatible with the prior negative search for SO_3 on Io by *Nelson and Smythe* [1986], although *Khanna et al.* challenge the spectral assignments of *Nelson and Smythe*.

The importance of SO_2-rock interactions is dependent on crustal recycling, which governs the probability of burial of SO_2 to temperatures where thermochemical reactions such as (R7) can occur [*Burnett*, 1995]. It is also necessary that SO_2 and silicate be in contact, but a compensating feature is that it is likely to be hot where silicate is found in the crust of Io today. There will be a tendency for hot silicate regions to drive off SO_2 prior to contact, but in regions of high crustal strength, e.g., in lava tubes or shallow intrusions, SO_2 and silicate material can be brought into contact for sufficient times at higher temperatures (approaching silicate magmatic temperatures) for SO_2 alteration to occur. The silicate flows seen in thermal infrared observations [e.g., *Blaney et al.*, 1995] must be relatively large to be detected. If size is correlated with rapid flow rate, then SO_2-bearing crustal regions can be overrun before the SO_2 is outgassed, providing for SO_2-rock interaction at the base of the flow. However, given the relatively low surface pressures, even around vents, and the ease with which SO_2 can escape a hot surface, it appears unlikely that the upper surfaces of fresh flows would be altered. Thus a high spatial resolution spectrum of a fresh (i.e., before being resurfaced with deposits) flow should look like silicate glass.

It is a concern that Na_2SO_4 was only confirmed with the soda-lime glass which is not a natural glass sample. There seems to be a preference for Ca or Fe sulfate formation from SO_2-rock interactions when these elements are present. This preference was also present, but less evident, in the oxidizing experiments (see discussion by *Johnson and Burnett* [1993]). In general the S-rich surface of Io and the absence of Fe ions in the Io torus are major constraints on the evolution of the planet. The very low reaction rate of the AbOr composition has inhibited detailed characterization; however, the observation of an oxidized S XPS peak undoubtedly means that an alkali sulfate was formed, as Na and K are the only sulfate-forming cations for this composition. The problem of reaction rate is ours. Continuous igneous activity and crustal recycling has been happening on the 10^9 year timescale on Io, so SO_2 alteration of a granitic crust on Io forming Na and K sulfates is a distinct possibility.

The total amount of Na_2SO_4 produced need not be large. For a global Na loss rate of 10^{26}-10^{27} s^{-1} [*Cheng et al.*, 1986], the production of Na_2SO_4 need only be ~10^8 atoms/(cm^{-2} s) in order to compensate for sputtering losses. This corresponds to only 10^{-12} g Na/yr per kilometer of crustal thickness. With this low required production rate, the primary reaction mechanisms need not be efficient, and occasional contact of SO_2 and hot silicate may be sufficient.

It is possibly significant that S is a reaction product of SO_2-rock interaction. There is no constraint on the ratio of S to SO_2 on Io; however, if the amount of Na-S-O phases on Io is much less than the amount of elemental S, as is likely, another source of elemental S is required. On Earth, SO_2 is a prominent volcanic volatile with S having a subordinate role. Although Io could be different in having a large amount of primary magmatic S, the decomposition of SO_2 by plasma-chemical interactions is probably the best method to produce elemental S.

Acknowledgments. We thank A. S. McEwen and an anonymous reviewer for thorough reviews. This research was supported by NASA NAGW 35-34 (D. Burnett) and NAGW 38-83 (S. Epstein). Caltech contribution 5914.

References

Ballester, G.E., D.F. Strobel, H.W. Moos, and P.D. Feldman, The atmospheric abundance of SO_2 on Io, *Icarus, 88*, 1-23, 1990.

Belcher, J., Low energy plasma in the Jovian magnetosphere, in *Physics of the Jovian Magnetosphere*, edited by A.J. Dessler, pp. 68-105, Cambridge Univ. Press, New York, 1983.

Blaney, D.L., T.V. Johnson, D.L. Matson, and G.J. Veeder, Volcanic eruptions on Io: Heat flow, resurfacing and magma composition. *Icarus, 113*, 220-225, 1995.

Burnett, D.S., Competition between Na_2SO_4 and Na sulfide in the upper crust of Io, *J. Geophys. Res., 100*, 21,265-21,270, 1995.

Carroll, M.R., and M.J. Rutherford, Sulfide and sulfate saturation in hydrous silicate melts, *Proc. Lunar Planet. Sci. Conf. 15th*, part 2, *J. Geophys. Res., 90*, suppl., C601-C612, 1985.

Carroll, M.R., and M.J. Rutherford, The solubility of igneous anhydrite; experimental results and implications for S behavior in the 1982 El Chichon trachyandesite and other evolved magmas, *J. Petrol., 28*, 781-801, 1987.

Carroll, M.R., and J.D. Webster, Solubilities of sulfur, noble gases, nitrogen, chlorine, and fluorine in magmas, *Rev. Mineral., 30*, 231-271, 1994.

Cheng, A.F., P. Haff, R.E. Johnson, and L.J. Lanzerotti, Interactions of planetary magnetospheres with icy satellite surfaces, in *Satellites*, edited by J.A. Burns and M.S. Matthews, pp. 682-721, Univ. of Ariz. Press, Tuscon, 1986.

Deer, W.A., R.A. Howie, and J. Zussman (Eds.), *An Introduction to the Rock-Forming Minerals*, 528 pp., Longman Group, Harlow, Essex, England, 1966.

Fanale, F, W.B. Banerdt, L.S. Elson, T.V. Johnson, and R.W. Zurek. Io's surface: its phase composition and influence on Io's atmosphere and Jupiter's magnetosphere, in *Satellites of Jupiter*, edited by D. Morrison, Univ. of Ariz. Press, Tuscon, 1982.

Feldman, L.C., and J.W. Mayer. *Fundamentals of Surface and Thin Film Analysis*. North-Holland, New York, 1986.

Gehrels, N., and E.C. Stone, Energetic O and S ions in the Jovian magnetosphere and their contribution to auroral excitation, *J. Geophys. Res., 88*, 5537-5550, 1983.

Gladney, E.S., and I. Rowlandts, 1987 compilation of elemental concentration data for USGS BHVO-1, MAG-1, QLO-1, RGM-1, SCo-1, SDC-1, SGR-1 and STM-1, *Geostand. Newsl. 12*, 253-362, 1988.

Hapke, B., The surface of Io: A new model, *Icarus, 79*, 56-74, 1989.

Johnson, M.L., and D.S. Burnett, Igneous origin for the Na in the cloud of Io, *Geophys. Res. Lett., 17*, 981-984, 1990.

Johnson, M.L. and D.S. Burnett, SO_2 weathering on Io (abstract), *Lunar Planet. Sci., XXII*, 649-650, 1991.

Johnson, M.L., and D.S. Burnett, SO_2-rock interaction on Io: reaction under highly oxidizing conditions, *J. Geophys Res. 98*, 1223-1230, 1993.

Johnson T.V., and D.L. Matson, Io's tenuous atmosphere, in *Origin and*

Evolution of Planetary and Satellite Atmospheres, edited by S. Atreya, J. Pollack, and M. Matthews, pp. 666-681, Univ. of Ariz. Press, Tuscon, 1989.

Khanna, R.K., J.C. Pearl, and R. Dahmani, Infrared spectra and structure of solid phases of SO_3: Possible identification of solid SO_3 on Io's surface. *Icarus 115*, 250-257, 1995.

Krimigis, S.M., and E.C. Roelof, Low energy particle population, in *Physics of the Jovian Magnetosphere*, edited by A.J. Dessler, pp. 106-156, Cambridge Univ. Press, New York, 1983.

Kumar, S., and D.M. Hunten, The atmospheres of Io and the other satellites, in *Satellites of Jupiter*, edited by D. Morrison, pp. 782-806, Univ. of Ariz. Press, Tucson, 1982.

Lellouch, E., M. Belton, I. dePater, S. Gulkis, and T. Encrenaz, Io's atmosphere from microwave detection of SO_2, *Nature, 346*, 639-641, 1990.

McEwen, A.S., and J.I. Lunine, Comment on "The surface of Io: A new model" by B. Hapke, *Icarus, 75*, 450-478, 1989.

Moses, J.I., and D.B. Nash, Phase transformations and the spectral reflectance of solid sulfur: Can metastable sulfur allotropes exist on Io?, *Icarus 89*, 277-304, 1991.

Nash, D.B. and J.I. Moses, Vacuum weathering of sulfur: temperature effects and applications to Io, *Geophys. Res. Lett. 15*, 697-700, 1988.

Nash, D.B., M.H. Carr, J. Gradie, D.M. Hunten, and C.F. Yoder, Io, in *Satellites*, edited by J.A. Burns and M.S. Matthews, pp. 629-688, Univ. of Ariz. Press, Tucson, 1986.

Nelson, R.M., and W.D. Smythe, Spectral reflectance of solid SO_3 (0.25-5.2 microns): Implications for Jupiter's satellite Io, *Icarus, 66*, 181-187, 1986.

Newman, S., S. Epstein, and E. Stolper, Water, carbon dioxide, and hydrogen isotopes in glasses from the ca. 1340 A.D. eruption of the Mono Craters, California: Constraints on degassing phenomena and initial volatile content, *J. Volcanol. Geotherm. Res., 35*, 75-96, 1988.

Schardt, A.W., and C.K. Goertz, High energy particles, in *Physics of the Jovian Magnetosphere*, edited by A.J. Dessler, pp. 157-196, Cambridge Univ. Press, New York, 1983.

Spencer J.R. and Schneider N.M. Io on the eve of the Galileo mission, *Ann. Rev. Earth. Planet. Sci., 24*, 125-190, 1996.

Summers, M.E. and D.F. Strobel, Photochemistry and vertical transport in Io's atmosphere and ionosphere, *Icarus, 120*, 290-316, 1996.

Trafton, L.M., J.J. Caldwell, C. Barnet, and C.C. Cunningham, The gaseous sulfur dioxide abundance over Io's leading and trailing hemispheres: HST spectra of Io's $C\ ^1B_2$-$X\ ^1A_1$ band of SO_2 near 2100Å, *Astrophys. J., 456*, 384-392, 1996.

Vogt, R.E., et al., Voyager 1: Energetic ions and electrons in the Jovian magnetosphere, *Science, 204*, 1003-1007, 1979.

Wagner, C.D. and G.E. Muilenberg (eds.), *Handbook of X-Ray Photoelectron Spectroscopy*, Perkin-Elmer Corp., Physical Electronics Division, Eden Prairie, MN, 1979.

D. S. Burnett, S. Eptstein, and J. Goreva, Division of Geological and Planetary Sciences, California Institute of Technology, MS 100-23, Pasadena, CA 91125. (e-mail: burnett@gps.caltech.edu; epstein@gps.caltech.edu; julia@gps.caltech.edu)

S. L. Haldemann, Department of Chemistry, University of California, Los Angeles, CA 90024. (e-mail: slh@chem.ucla.edu)

M. L. Johnson, Gemological Institute of America, Carlsbad, CA 92008. (e-mail: mjohnson@alumni.caltech.edu)

A. Rice, Division of Physics, Mathematics and Astronomy, California Institute of Technology, MS 200-36, Pasadena, CA 91125. (e-mail: rice_a@caltech.edu)

(Received July 8, 1996; revised February 25, 1997; accepted March 10, 1997.)